

# Verification of DUNE solver for heat equation

Peter Meisrimel

October 2, 2020

## Contents

<b>1</b>	<b>Verification of monolithic solver</b>	<b>2</b>
1.1	Time . . . . .	2
1.2	Space . . . . .	2
<b>2</b>	<b>Individual solvers</b>	<b>3</b>
2.1	Dirichlet solver . . . . .	3
2.1.1	Time . . . . .	3
2.1.2	Space . . . . .	4
2.2	Neumann solver . . . . .	5
2.2.1	Time . . . . .	5
2.2.2	Space . . . . .	5
<b>3</b>	<b>Waveform relaxation (WR)</b>	<b>6</b>
3.1	Tolerance . . . . .	6
3.2	Time . . . . .	7
3.3	Space . . . . .	8
3.4	Self consistency . . . . .	9
3.5	Optimal relaxation parameter . . . . .	10
3.6	Conclusion . . . . .	11

Note, these were mostly done for myself as means of verifying correctness of the solver and require more detailed descriptions.

Besides basic verification, I also do a comparison of two different methods for computing the heat flux. The first one being  $\nabla \mathbf{u} \cdot \mathbf{n}$ , i.e., the straight forward one via the solution in a given point. The second one is obtained via the classical Domain Decomposition approach, see Azahars papers. In the following plots, I will refer to the first method as "**grad**" and the second one as "**weak**". For easy comparison, I'll display them side by side, "grad" on the left and "weak" on the right.

## 1 Verification of monolithic solver

### 1.1 Time

Time integration error using 64 internal unknowns per unit length. See Figure 1, first, resp. second orders are observed.

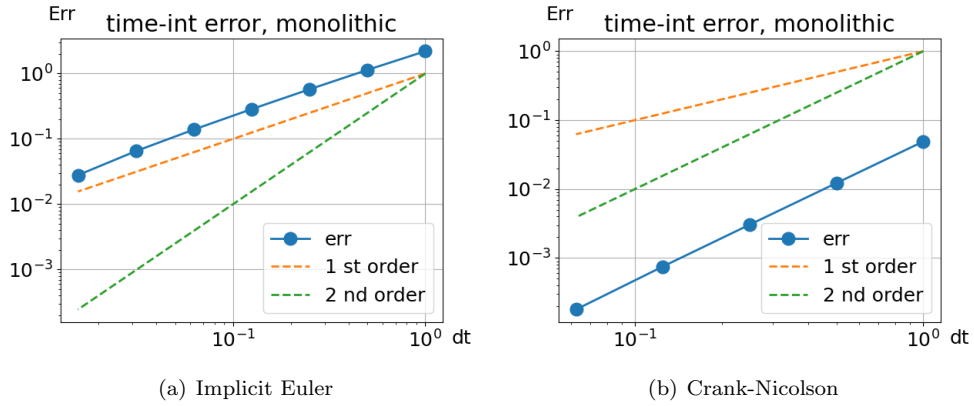


Figure 1: Time integration error, monolithic.

### 1.2 Space

L2 error in space, using 2nd order time-integration and sufficiently many timesteps. See Figure 2, second order observed.

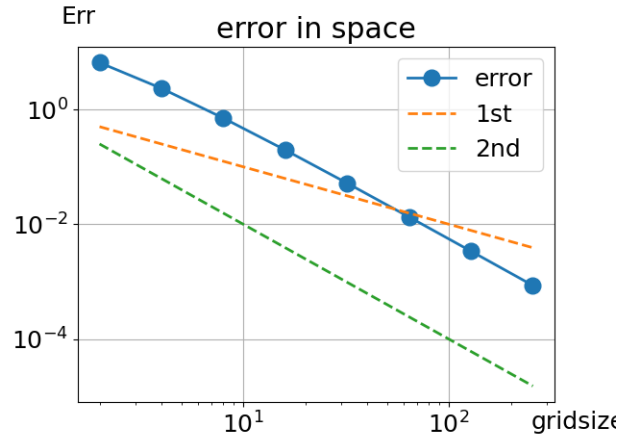


Figure 2: Space error of monolithic solver.

## 2 Individual solvers

We first verify the correctness of the Dirichlet and Neumann solvers on themselves, using exact values for the boundaries.

### 2.1 Dirichlet solver

#### 2.1.1 Time

See Figures 3 and 4, first, resp. second order is observed, stagnates upon hitting the spatial error limit. The heat flux computed by "Grad" appears to have a smaller error in space.

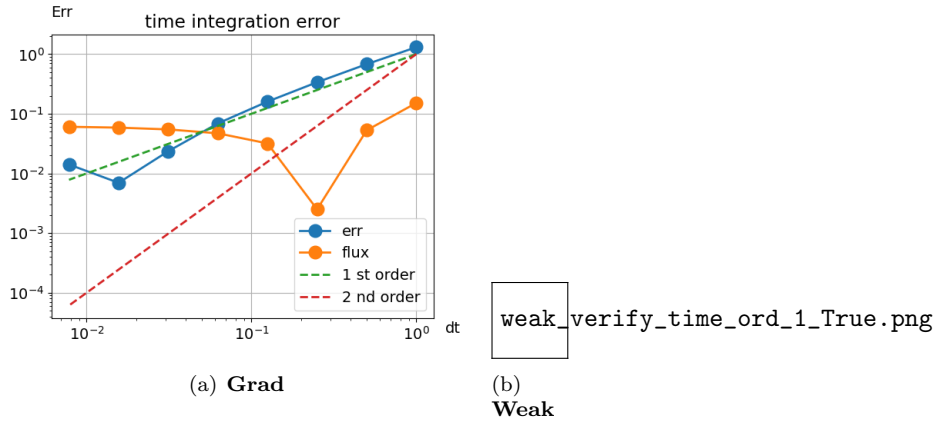
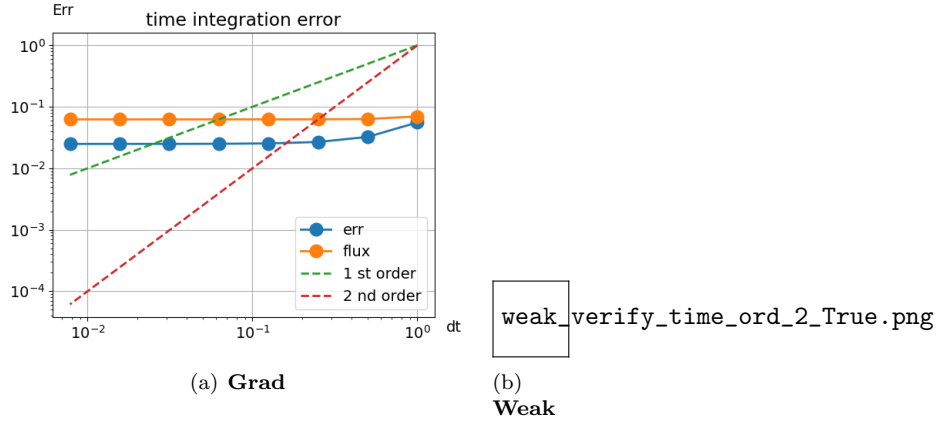
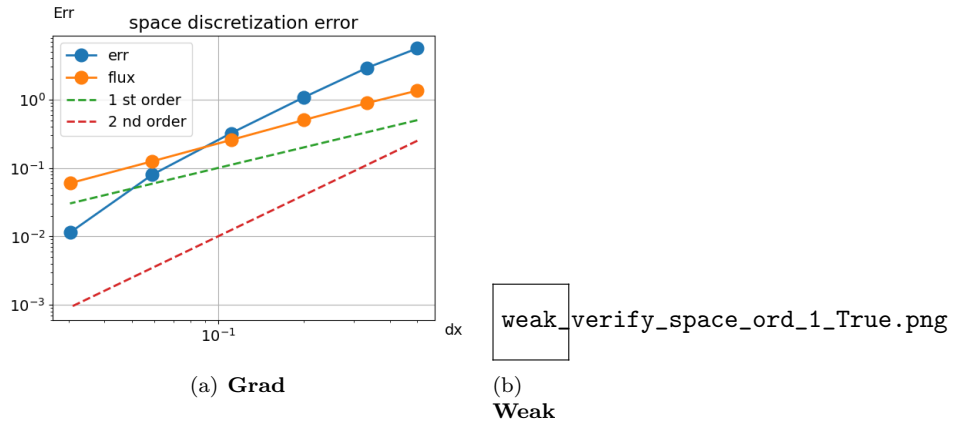


Figure 3: Time integration error, Dirichlet solver, Implicit Euler.



### 2.1.2 Space

See Figures 5 and 6. Second order in the solution is observed, stagnates a bit too early for IE due to hitting limit of time-integration error. Flux is at most first order accurate due to being the derivative of the solution, curiously enough, it appears to be of order 1/2 for "Weak" & Implicit Euler.



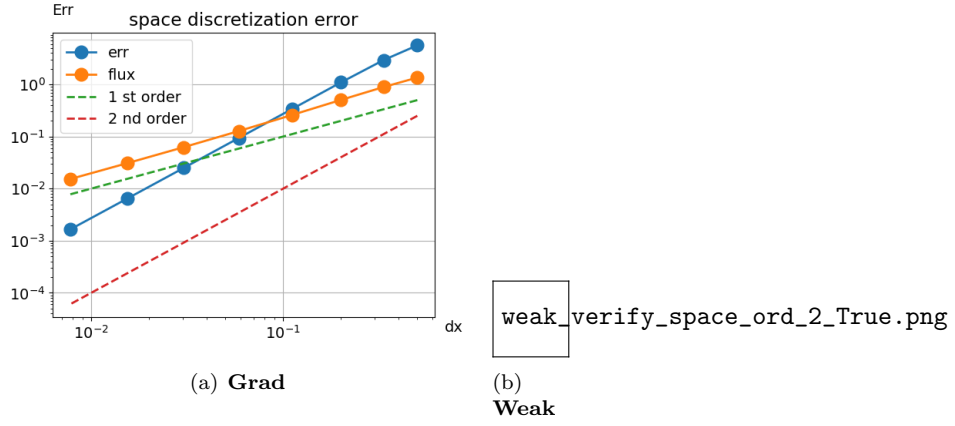


Figure 6: Space discretization error, Dirichlet solver, Crank-Nicolson.

## 2.2 Neumann solver

Note that the different variants of computing the flux do not concern the Neumann solver.

### 2.2.1 Time

See Figure 7, first, resp. second order is observed.

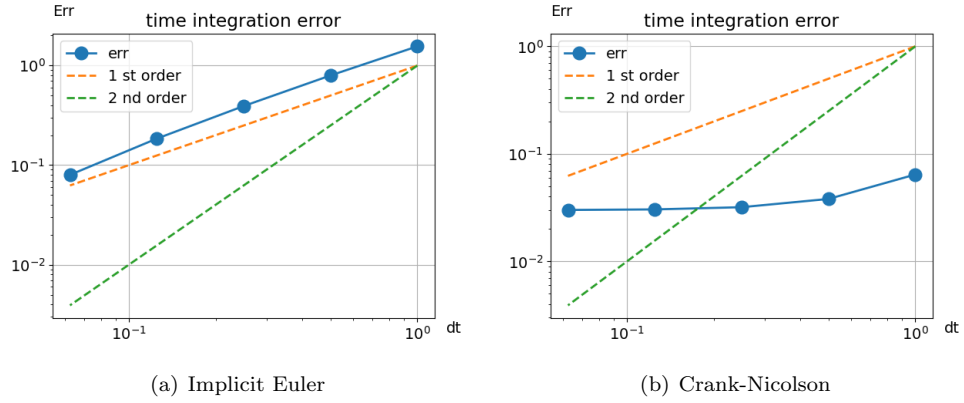


Figure 7: Time integration error, Neumann solver.

### 2.2.2 Space

See Figure 8. Second order in the solution is observed, stagnates a bit too early for IE due to hitting limit of time-integration error.

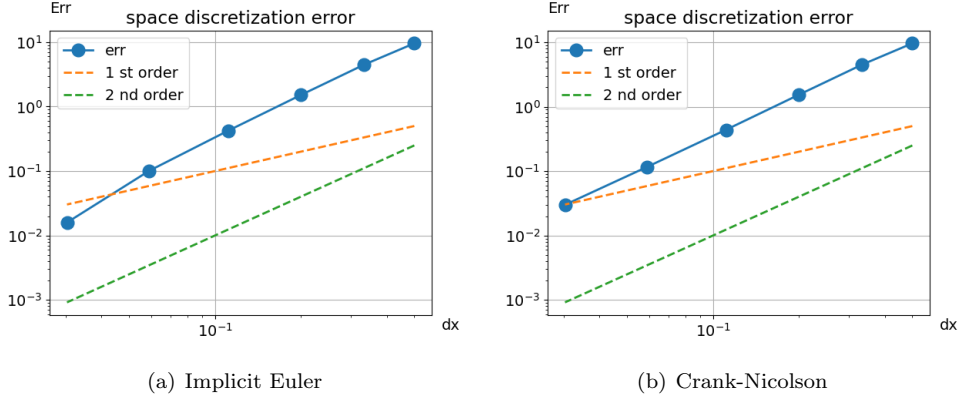


Figure 8: Space discretization error, Neumann solver.

### 3 Waveform relaxation (WR)

The general question is if the solution obtained from using WR converges to the monolithic solution. Our key parameters to control are  $\Delta t$ ,  $\Delta x$  and  $TOL$ , the tolerance used for the termination criterion in the WR. In the following test we vary one while keeping the other 2 fixed.

#### 3.1 Tolerance

We want to see that the solution from using WR converges to the monolithic solution for  $TOL \rightarrow 0$ . Result can be seen in Figures 9 and 10. We do not observe convergence. At this point, we can assume that the data exchange due to WR introduces an error in time or space.

The flux computation via "Weak" yields a notably smaller error.

The non-convergence means the monolithic solution is not the fixed point of WR, for fixed  $\Delta t$ ,  $\Delta x$  and  $TOL \rightarrow 0$ .

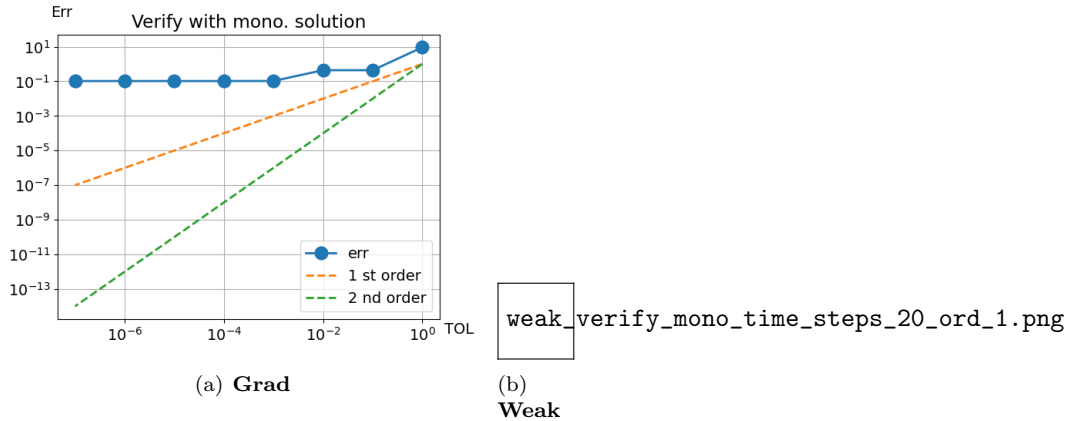
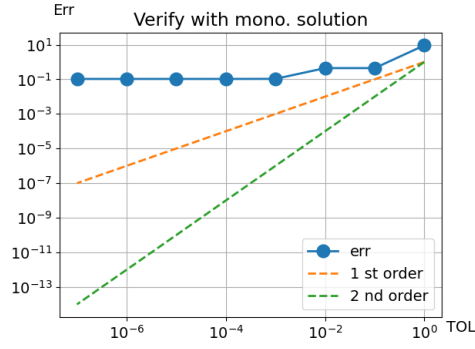


Figure 9: WR for  $TOL \rightarrow 0$ . Implicit Euler.



(a) **Grad**

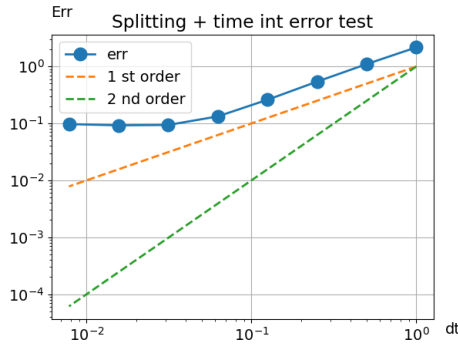
weak\_verify\_mono\_time\_steps\_20\_ord\_2.png

(b) **Weak**

Figure 10: WR for  $TOL \rightarrow 0$ . Crank-Nicolson.

### 3.2 Time

Next up we take  $TOL = 10^{-10}$  and let  $\Delta t \rightarrow 0$ . See Figures 11 and 12 for results. For implicit Euler, one gets a clear first order convergence rate. With Crank-Nicolson, second order is observed, with the addition that flux computation using "Grad" leads to early stagnation, possibly due to the spatial error.



(a) **Grad**

weak\_verify\_comb\_error\_ord\_1.png

(b) **Weak**

Figure 11: WR for  $\Delta t \rightarrow 0$ . Implicit Euler.

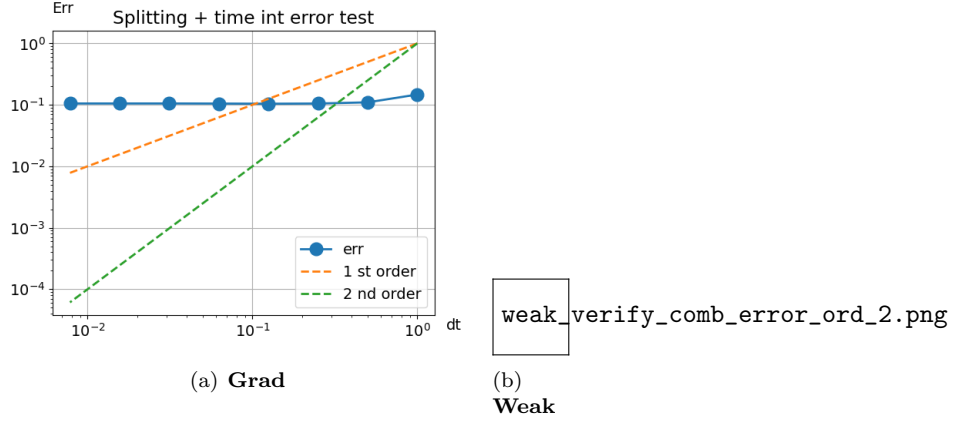


Figure 12: WR for  $\Delta t \rightarrow 0$ . Crank-Nicolson.

### 3.3 Space

Lastly, we consider  $\Delta x \rightarrow 0$  with  $\Delta t$  fixed and  $TOL = 10^{-10}$ . There should not be any error when comparing with the monolithic solution. However, there is a discrepancy due to not exactly having a matching discretization. Data exchange on the interface is discrete, but the input is a continuous (in space) function. This apparently introduces an additional error, which ideally vanishes as quickly as possible for  $\Delta x \rightarrow 0$ .

See Figures 13 and 14 for results. For "Grad" we observe first order convergence, presumably because the computed flux is only first order accurate in space. With "Weak" we observe second order for implicit Euler and close to 4th order for Crank-Nicolson.

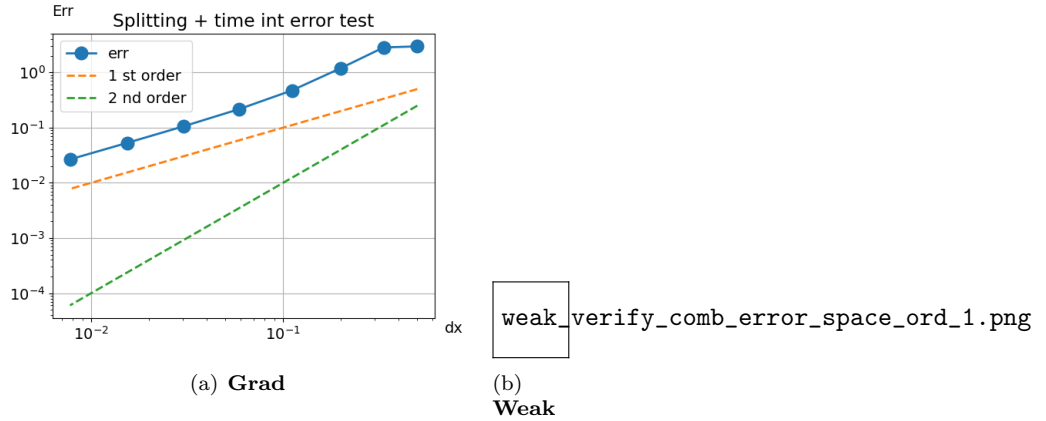


Figure 13: WR for  $\Delta t \rightarrow 0$ . Implicit Euler.



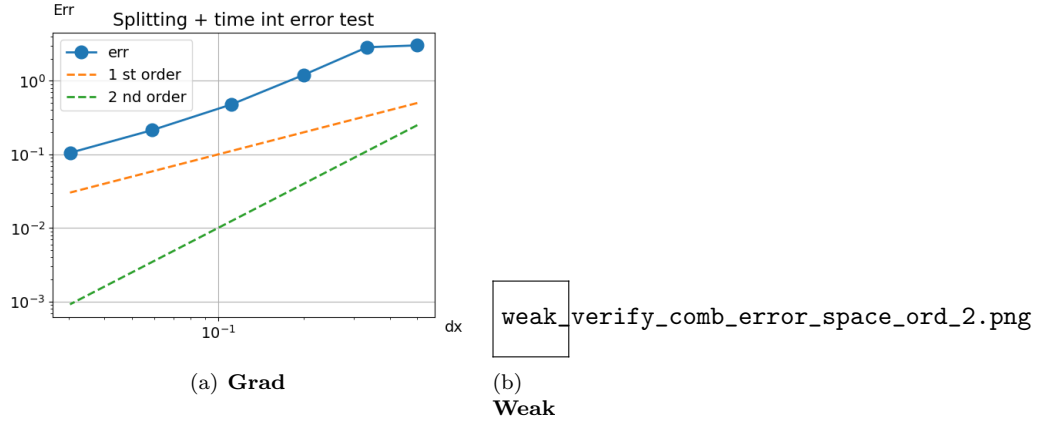


Figure 14: WR for  $\Delta t \rightarrow 0$ . Crank-Nicolson.

### 3.4 Self consistency

While we observe an additional error in space due to WR, our main goal is to resolve the time-coupling. Thus the question is if the order in time is preserved. We verify repeating the verification of  $\Delta t \rightarrow 0$  and instead measure the error using a reference solution for a sufficiently small timestep. Figures 15 and 16 show the results, which is that the time-integration orders are preserved.

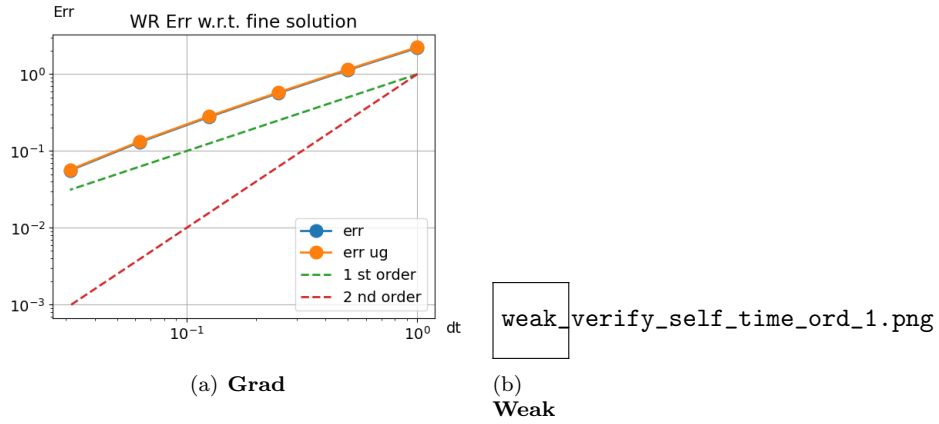


Figure 15: WR for  $\Delta t \rightarrow 0$  using reference solution with smaller  $\Delta t$ . Implicit Euler.

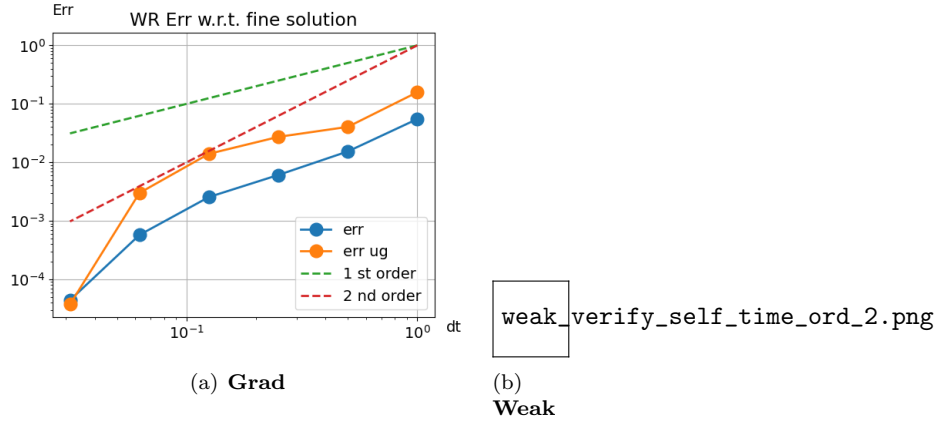


Figure 16: WR for  $\Delta t \rightarrow 0$  using reference solution with smaller  $\Delta t$ . Crank-Nicolson.

### 3.5 Optimal relaxation parameter

Here we want to verify the optimal relaxation parameter being  $\Theta = 1/2$  for equal material parameters. Results in Figures 17 and 18 look good.

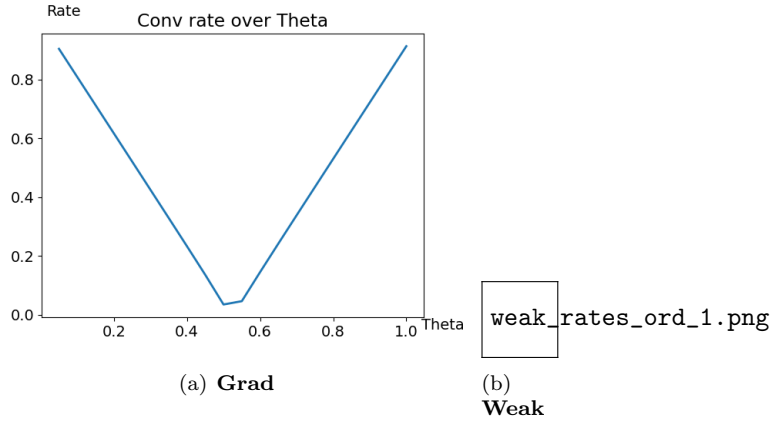


Figure 17: Observed convergence rates. Implicit Euler.

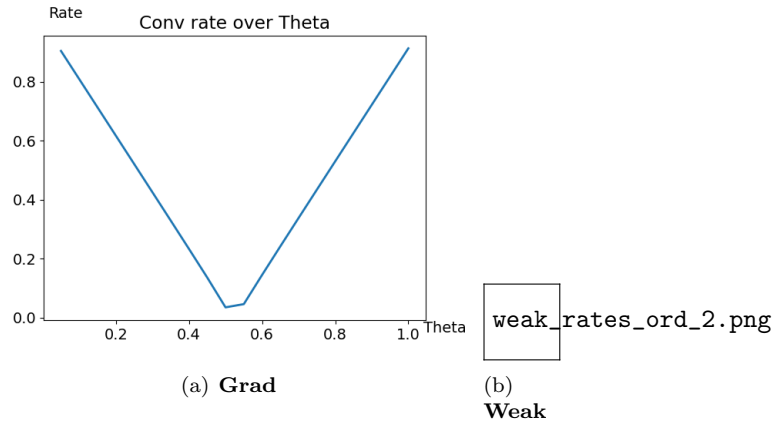


Figure 18: Observed convergence rates. Crank-Nicolson.

### 3.6 Conclusion

The expected orders are attained. While flux computation via the gradient ("Grad") yields an objectively better result for the Dirichlet solver on its own, the flux computed via the weak form ("Weak") yields better results in the context of Waveform-Relaxation.